Volume 8
Number 5
7 February 2020
Pages 829–1072

Journal of Materials Chemistry B

Materials for biology and medicine

rsc.li/materials-b

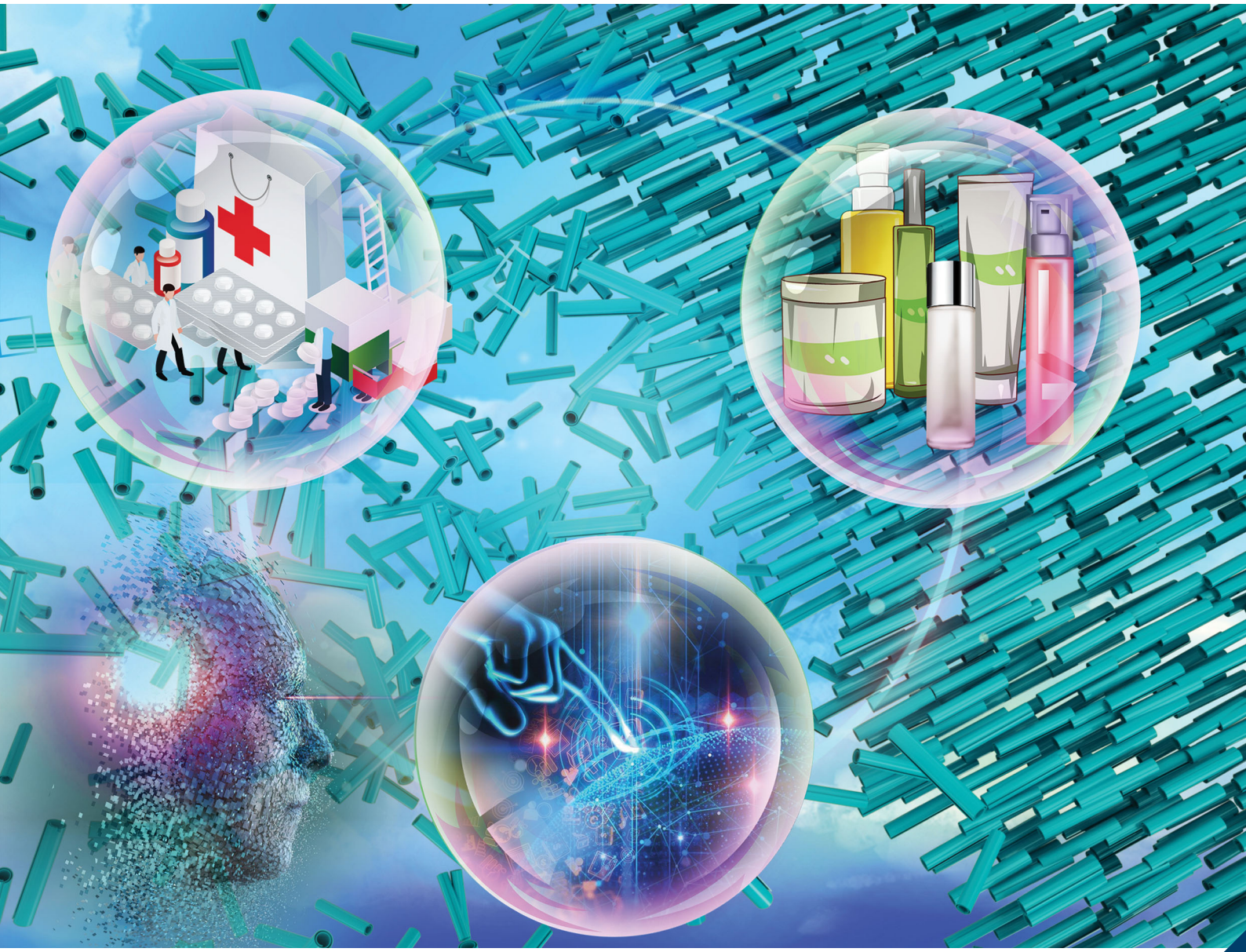

ISSN 2050-750X

ROYAL SOCIETY OF CHEMISTRY

REVIEW ARTICLE

Mingxian Liu *et al.*

Self-assembled structures of halloysite nanotubes: towards the development of high-performance biomedical materials

Indexed in Medline!

Journal of Materials Chemistry B

ROYAL SOCIETY OF CHEMISTRY

REVIEW

View Article Online
View Journal | View Issue

Cite this: *J. Mater. Chem. B*, 2020, **8**, 838

Self-assembled structures of halloysite nanotubes: towards the development of high-performance biomedical materials

Xiujuan Zhao, Changren Zhou and Mingxian Liu *

Received 3rd November 2019,
Accepted 3rd December 2019

DOI: 10.1039/c9tb02460c

rsc.li/materials-b

Halloysite nanotubes (HNTs), 1D natural tubular nanoparticles, exhibit a high aspect ratio, empty lumen, high adsorption ability, good biocompatibility, and high biosafety, which have attracted researchers' attention in applications of the biomedical area. HNTs can be readily dispersed in water due to their negatively charged surface and good hydrophilicity. The unique rod-like structure and surface properties give HNTs assembly ability into ordered hierarchical structures. In this review, the self-assembly approaches of HNTs including evaporation induced self-assembly by a "coffee-ring" mechanism, shear force induced self-assembly, and electric field force induced self-assembly were introduced. In addition, HNT self-assembly on polymeric substrates and biological substrates including hair, cells, and zebrafish embryos was discussed. These assembly processes are related to noncovalent interactions such as electrostatic, hydrogen bonding, and van der Waals forces or electron-transfer reactions. Moreover, the applications of self-assembled HNT patterns in biomedical areas such as capture of circulating tumor cells, guiding oriented cell growth, controlling cell germination, and delivery of drugs or nutrients were discussed and highlighted. Finally, challenges and future directions of assembly of HNTs were introduced. This review will inspire researchers in the design and fabrication of functional biodevices based on HNTs for tissue engineering, cancer diagnosis/therapy, and personal healthcare products.

1. Introduction

Nanoparticles have attracted much interest with the unique small size effect, high surface area effect and quantum size effect. They have been widely applied in the modern medical and other commercial fields. One-dimensional (1D) nanoparticles including nanotubes, nanowires, nanofibers, nanobelts, or nanorods have a high aspect ratio and anisotropy, which give them excellent mechanical, electrical and magnetic properties.[1] Among 1D nanoparticles, halloysite nanotubes (HNTs) are a natural clay mineral with a high aspect-ratio and hollow tubular structure.

Department of Materials Science and Engineering, Jinan University, Guangzhou 510632, China. E-mail: liumx@jnu.edu.cn

Xiujuan Zhao

Xiujuan Zhao received her PhD from the Department of Biomedical Engineering, School of Materials Science and Engineering, South China University of Technology in 2016. Currently she is doing post-doctoral work at Jinan University. Her research focuses on polysaccharides and halloysite nanotubes for biomedical applications.

Changren Zhou

Professor Changren Zhou is a doctoral tutor of biomedical engineering of Jinan University. He graduated from department of chemistry Shandong University after graduating from school to teach in 1981. He received a PhD from Sun Yat-sen University in 1993. He has served as a biomedical engineering researcher from 1993 to the present. His main research areas are tissue engineering, biodegradable materials, blood compatible materials, nano materials and biomaterials processing.

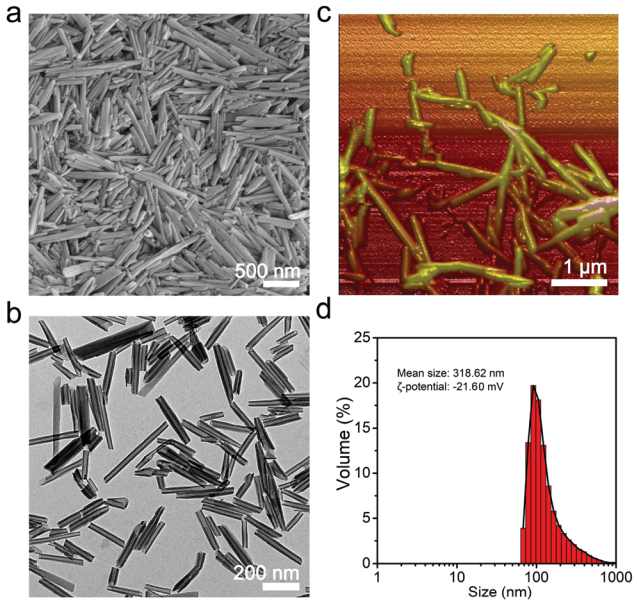

Fig. 1 Morphology of HNTs characterized by SEM (a), TEM (b) and AFM (c); nanoparticle size and zeta potential (d).

Their chemical formula is $Al_2Si_2O_5(OH)_4{\cdot}nH_2O$. Generally, the length of HNTs is from 200 nm to 2 μm. Their outer diameter and inner diameter are in the range of 50–70 and 10–20 nm respectively. Interestingly, HNTs are charged positively and negatively due to the Al_2O_3 and SiO_2 in the inner and outer surface of the nanotubes.[2,3] Raw halloysite mineral is abundantly deposited in the world such as in the United States, China, New Zealand, Australia, Poland, and Brazil. In China, many provinces including Henan, Hunan, Guizhou, Jiangsu, Shanxi, and Yunnan have halloysite mineral deposits. There are reserves estimated at 100 million tons of halloysite raw material in China. Due to the overall negative charges, there exists a repulsion force among the tubes, which leads to good aqueous dispersion.[4] Morphology and particle size characterizations of HNTs are presented in Fig. 1. HNTs can exhibit high mechanical properties, adsorption capacity, dispersion stability, and biocompatibility.[5] In the biomedical field, HNTs are widely used in tissue engineering scaffolds, wound healing dressings, drug delivery, and biosensors.[6–8]

Self-assembly of nanoparticles is an important aspect in nanotechnology, since it can be employed to design and fabricate functional devices towards the development of practical applications of nanoparticles. 1D nanoparticles are easily tunable for arrangement as the building blocks of self-assembled architectures. Up to now, a lot of 1D nanoparticles, such as carbon nanotubes, gold nanorods, Ag nanowires, cellulose nanocrystals, and HNTs have been used to prepare structural materials by self-assembly.[9–12] In recent decades, a variety of strategies were explored for the self-assembly of 1D nanoparticles. Usually, the methods of self-assembly of 1D nanoparticles can be divided into two types: capillary force induced assembly and external field mediated assembly. Capillary force induced assembly can be performed in normal condition and confined space. The external fields used for assembly contain shear stress, electric fields, magnetic forces, and so on.[12,13] In the last few years, many studies on the self-assembly of HNTs were reported and critical progress was made.[11,14] The successful assembly of HNTs relies on obtaining stable dispersions of the nanotubes in solvents such as water and polymer solutions. The excellent hydrophilic property and high surface zeta potential brought by the massive hydroxyl groups and different inner/outer chemical composition facilitate HNT self-assembly methods. At present, the studies of HNT self-assembly mainly focused on the solvent evaporation method in a confined space, shear force induced nanotube assembly, electric force induced assembly, assembly on polymer substrates and assembly on biological substrates.

For biomedical applications, the biocompatibility and potential toxicity of HNTs in vivo are most important and need to be systematically assessed. Previously, a *Caenorhabditis elegans* model and zebrafish experiments of HNTs were used to evaluate the toxicity of HNTs, which suggested that HNTs have very low toxicity.[15,16] HNTs can find applications in various biomedical areas including drug delivery, tissue engineering scaffolds, cell capture, and wound healing materials and their biocompatibility was confirmed in different cell lines.[17] The assembled structures of HNTs such as regular patterns with anisotropy, high nanotube alignment, and easily functionalized hydroxyl groups contribute interesting results in biomedical applications. For example, cancer cells can recognize the HNT pattern substrate and respond to the chemical and morphological characteristics of the rough surfaces *via* ''material–cell'' interaction. The aligned HNT architecture can induce the oriented growth of fibroblasts and stem cells, which can further promote their migration, proliferation and differentiation. Polymer or biological surfaces decorated with HNTs show promising application in tissue engineering, disease detection, and healthcare. Therefore, it is very worthy and necessary to review the advance of the assembly techniques and their corresponding biomedical applications of HNTs in the field of soft tissue diseases.

In this review, we focus on HNT self-assembly and their biomedical applications. The recent developments of HNT self-assembly techniques were firstly presented. The understanding

Mingxian Liu

Mingxian Liu received his BS degree from Qingdao University of Science & Technology in 2004, and PhD in materials science from the South China University of Technology in 2010. After that, he worked as an assistant professor in the Department of Materials Science and Engineering at Jinan University and became a full professor of biomaterials there in 2016. The research interest of his lab is centered on natural nanomaterials (i.e. halloysite nanotubes and chitin nanocrystals) aimed at biomedical applications in tissue engineering, drug delivery, biosensors, and so on.

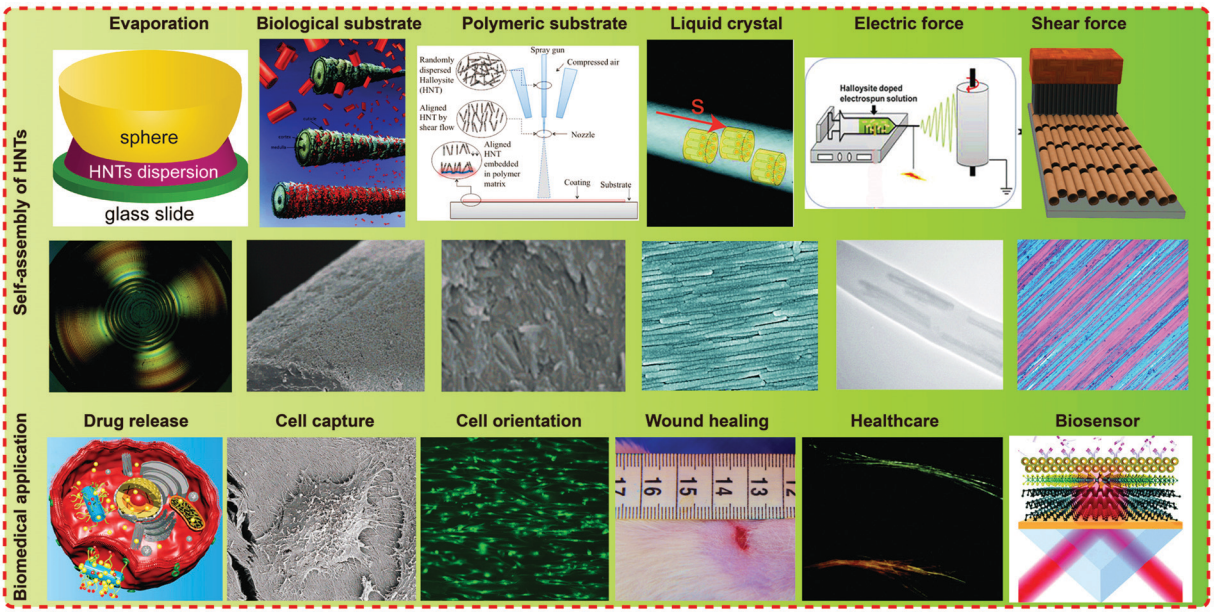

Fig. 2 Self-assembly approaches of HNTs and their corresponding biomedical applications. Reproduced with permission from American Chemical Society, Royal Society of Chemistry, Wiley-VCH Verlag GmbH & Co. KGaA and Elsevier.[11,19,27,32,34,35,43,47,59,60]

of the formation of the pattern structure corresponding to the self-assembly method was illustrated. Then, the biomedical applications of HNT self-assembled structures were introduced. Especially, cell capture and self-assembled HNT substrate induced cell orientation were emphasized (Fig. 2). Finally, a brief perspective and challenges of HNT assembly were discussed. It is expected that more and more self-assembly methods of HNTs and their practical applications will be explored in the future.

2. Self-assembly methods of HNTs

2.1. Solvent evaporation induced HNT self-assembly

2.1.1. Dispersion property of HNTs. The stability of nanoparticle dispersions plays a key role in the self-assembly induced by solvent evaporation. The outer and inner surfaces of tubular HNTs are negatively and positively charged, respectively. The overall potential of HNTs is negative, which leads to the good dispersion of HNTs in water due to the repulsion of the nanoparticles.[18] The stable dispersion results in a single nanotube can be moved towards the solid–liquid–gas three-phase drying line.[19] However, in order to further improve the dispersion stability of HNTs in water, it is effective to use polystyrene sulfonate sodium (PSS) or sodium hexametaphosphate to modify the HNTs. The negative charge of the raw HNTs and PSS–HNT in water generates a ζ-potential value of -26.1 and -52.2 mV, respectively.[20] The much higher zeta potential is of benefit for the improvement of the dispersion stability. The influence of the surfactant on the dispersion of HNTs is systematically investigated by Fakhrullin *et al.*[21]

2.1.2. Droplet drying induced self-assembly *via* the "coffee-ring" effect. Solvent evaporation induced nanoparticle self-assembly holds advantages including simplicity, easy operation and low production cost, although it has disadvantages such that it can't be performed on a large scale. The "coffee-ring" effect can be used to explain the formation of the drying pattern structure. Specifically, an ordered ring structure can be formed at the pinned contact line when drying a droplet of a nanoparticle dispersion. This phenomenon is understood by the fact that the evaporation rate at the edge of the droplet is higher than that at the center of the droplet, which leads to a capillary force towards the edge and the flow brings the suspended particles from the center to the droplet edge.[22]

Several factors such as droplet volume, concentration, solvent type, drying temperature, surfactant, external field, and nanoparticle shape have a significant influence on the formation of the coffee-ring structure.[23] Yunker *et al.* studied the effects of nanoparticle shape on the "coffee-ring" formation. The spherical nanoparticles did not disturb the interface between the liquid and solid. But the oval-shaped nanoparticles had an effect on the interface between the liquid and solid, so that there was an attractive force among the oval-shaped nanoparticles which could compensate for the driving force of pulling the nanoparticles to the edge. With the evaporation of the solvent the oval-shaped nanoparticles were stuck. And then more and more nanoparticles were stuck and the nanoparticles were coated on the surface evenly.[24]

The first sample of a halloysite structure assembled as a coffee-ring deposit was reported in the year of 2014. Zhao *et al.* dropped a colloidal HNT dispersion onto a substrate. After drying at 65 °C, HNTs were aligned with orientation at the edge of the coffee-ring when the concentration of HNTs reached $\sim$0.05 mg mL^{-1}.[14] As shown in Fig. 3a, a "coffee-ring" deposit at the periphery was formed due to the outward capillary flow that occurred during the water evaporation. From Fig. 3b the contact line between the droplet and the substrate was pinned as the drop evaporated and the hydrodynamic flow into the

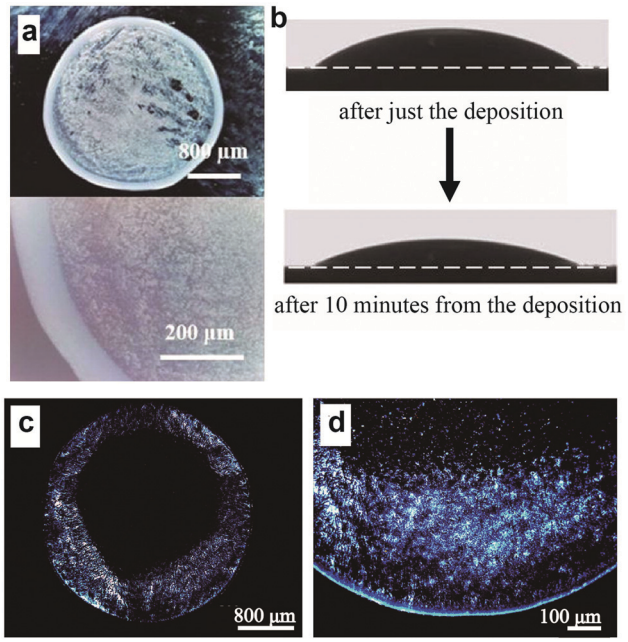

Fig. 3 Evaporation induced self-assembly of a PSS modified HNT dispersion on a silicon wafer. (a) Optical micrographs after the drying of the droplet; (b) the appearance difference of the PSS/HNT dispersion during the drying; polarized optical images of the PSS/HNT dispersion after drying (6 mg mL^{-1}, 65 °C, (c) whole view and (d) edge section). Reproduced with permission from ref. 14. Copyright 2015, Elsevier.

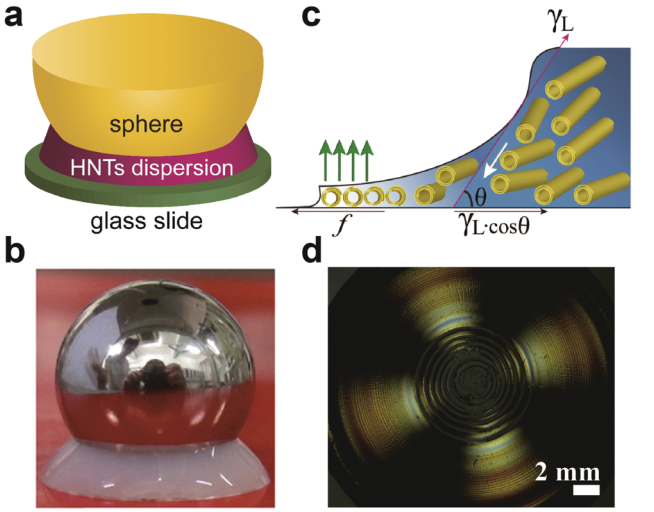

Fig. 4 Schematic illustration (a) and device photo (b) of the sphere–flat confined space; (c) schematic illustration of the thin meniscus formed at the three-phase contact line and the force balance (f is the frictional force generated by the HNT disposition at the contact line, towards the direction of the edge; due to the convective force the HNTs moved and resulted in γ_L and $\gamma_L \cdot \cos\theta$, with θ being the contact angle between the suspensions and the substrate); (d) polarized optical images of the HNT concentric ring pattern induced by evaporation. Reproduced with permission from ref. 19. Copyright 2017, American Chemical Society.

droplet drove the dispersed nanotubes to the edge, concentrating the suspension. According to Onsager's theory, when the concentration of anisotropic particles reaches a critical colloid concentration, the nanoparticles will align parallel to the edge and a liquid crystal phase can be found. The polarized optical images from Fig. 3c and d proved that a liquid crystal phase occurred when the concentration of HNTs was 6 mg mL^{-1}. Subsequently, Zhang *et al.* prepared a highly oriented HNT layer on a polyacrylonitrile porous membrane *via* a facile evaporation-induced method.[25,26] This simple coating method based on a HNT layer could lead to enhanced properties. For example, the composite membrane exhibited better selectivity for dye/salt solution and good water permeability, and excellent antifouling behavior against organic dyes and bovine serum albumin.

2.1.3. Solvent evaporation induced HNT self-assembly in a confined space. Our laboratory prepared highly ordered and concentric ring patterns consisting of HNTs with hierarchical cholesteric architectures by evaporation-induced self-assembly in a sphere-on-flat geometry[19] (Fig. 4a and b). A confined space was formed between a glass or stainless-steel sphere and glass slides. The capillary force and friction force balance of the HNT dispersion in the confined space could lead to a periodic pinning and depinning deposition process during the solvent evaporation. The frictional force f was generated due to the surface roughness, which can pin the solid–liquid–gas three phase contact line. But the capillary force (depinning force) pulled the liquid inward. As the solvent evaporating capillary force was larger than the pinning force and the contact line jumped the new position. Finally, a periodically ring pattern was formed. The width and thickness of the ring could be controlled by adjusting the concentration of the HNT dispersion and drying temperature.

Patterns with different shapes can be regulated by controlling the spatial distribution of the droplet. In order to get different HNT patterns, various confined spaces including glass capillary tubes, slit-like spaces, and pyramid–flat structures have been designed. For example, a strip-like HNT pattern on the inner surface of tubes walls was prepared by HNT assembly in glass capillary tubes which provided the confined space (Fig. 5a).[20] The HNT dispersion was dropped in a slit-like confined space composed of two glass slides and two gaskets. After drying, a strip-like structure from HNT self-assembly on the vertical substrate was obtained (Fig. 5b).[27] Similarly, the sphere in the sphere-on-flat model was replaced with a pyramid-shaped iron and a concentric square ring pattern was obtained (Fig. 5c). In conclusion, these confined spaces were easily constructed and low-cost, so solvent evaporation induced HNT self-assembly shows promising application in various areas.

2.2. Shear force induced HNT self-assembly

Using an external force such as shear force to drive the orientation of 1D nanoparticles is a very important strategy. Significant efforts have been made for the orientation of 1D nanoparticles using the shear force generated by fluid flow,[12] a polymer suspension,[28] a brush[11,29,30] and a blade.[31] Zan *et al.* directed 1D nanoparticles including tobacco mosaic virus, gold nanorods and bacteriophage M13 to align inside glass tubes by controlling the flow rate and the surface properties. Their research results showed that the flow rate, the nanoparticle concentration

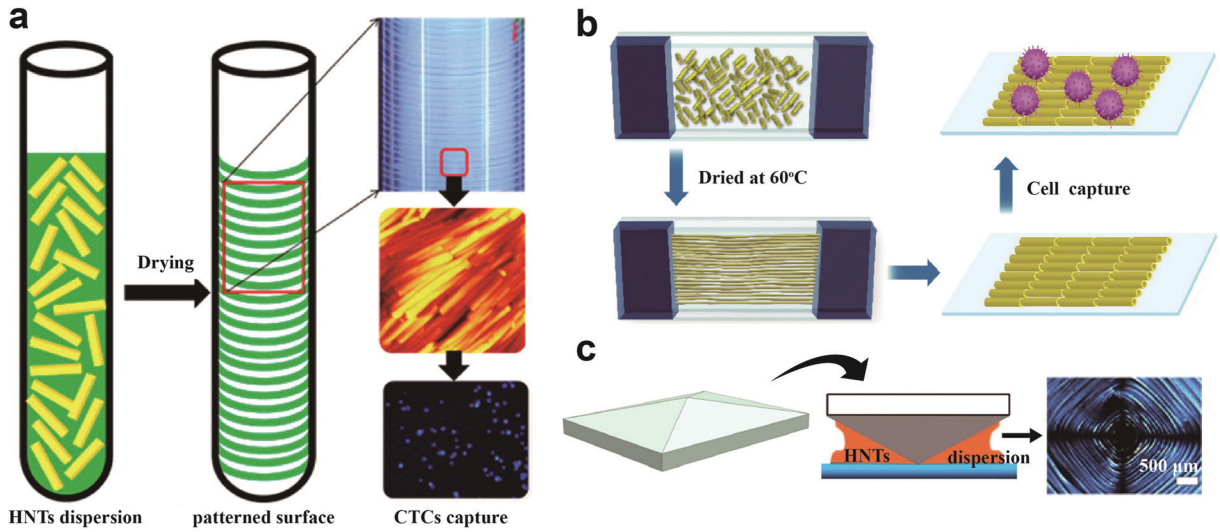

Fig. 5 (a) Preparation of stripe-like HNT patterns in glass capillary tubes for capture of tumor cells, reproduced with permission from ref. 20, Copyright 2016, American Chemical Society; (b) the preparation of a patterned HNT coating in a slit-like confined space, reproduced with permission from ref. 27, Copyright 2017, Royal Society of Chemistry; (c) preparation of a concentric square ring using the pyramid-shaped iron and glass slide, unpublished.

and properties such as the length and modulus had an effect on the orientation degree (Fig. 6a).[12] Chen *et al.* brushed a mixed suspension of hydroxyapatite mineral microfibers (HA) and sodium alginate (SA) along a hot planar substrate in a certain direction. An ordered film of HA/SA was formed and the orientation of HA microfibers was identified by the birefringence characteristics.[30]

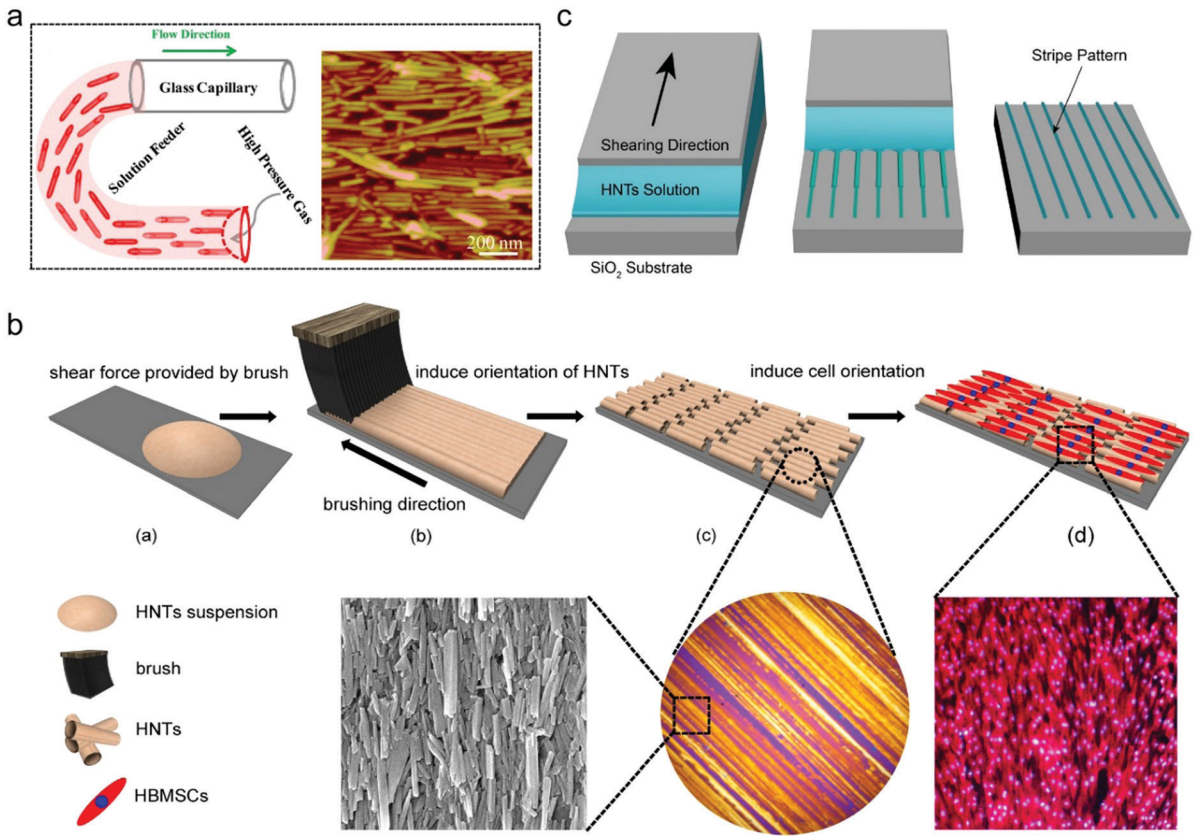

Fig. 6 (a) Schematic illustration of 1D nanoparticle orientation driven by fluid flow. A 1D nanoparticle solution was filled in the tubes and the nanoparticles flowed at a drive of high pressure gas. The AFM image showed good orientation of 1D nanoparticles.[12] Copyright 2013, American Chemical Society. (b) Schematic illustration of preparing oriented HNT arrays using a brush and guiding the cell orientation.[11] Copyright 2019, Wiley-VCH Verlag GmbH & Co. KGaA. (c) Formation of HNT stripe patterns under two parallel glass sheets, unpublished.

A simple method of driving a unidirectional HNT array is shown in Fig. 6b. HNTs were aligned by shear force in strip-like patterns accomplished with drying at elevated temperatures. The shear force was provided by a commercial brush. The results suggested that most HNTs could align along the direction of the shear force and the orientation of the HNTs depended on the concentration, substrate, brush type and temperature. This method was versatile, simple and did not need complicated instruments.[11]

The dispersion concentration, viscosity, drying temperature, hydrophilic of the substrates and aspect ratio of 1D nanoparticles play a significant role in the self-assembly.[11,12,30] For example, it was found that the HNT concentration affected the alignment of the tubes during assembly. When the HNT concentration was low there was not good tube orientation, which arose from the poor colloid stability and low viscosity. At low concentration the nanotube repulsion remained weak and led to HNT aggregation.[11] The shear force provided by the brush was also affected by the dispersion viscosity. At a 2% concentration of HNTs the viscosity was lower, which led to a weak shear force on the HNTs.[11,30] HNTs with low aspect ratio (α = 3.5) would suppress the "coffee-ring" effect, resulting in a uniform distribution without preferred alignment. However, HNTs with a very high aspect ratio (α = 13.2) could effectively produce a uniform oriented distribution on hydrophilic substrates.[25]

Our laboratory also tried to provide the shear force for HNT alignment using two parallel glass sheets (Fig. 6c). During the one glass sheet sliding, the HNT dispersion was subjected to shear force. Meanwhile, the glass substrate at the bottom was heated at 60 °C. Under the effects of the shear force and "coffee-ring" effect, oriented HNT stripes could be obtained.

It is know that liquid crystals can be ordered under an external force such as shear force, magnetic force, or electric force, and aligned macroscopic materials with outstanding properties can be obtained. Song *et al.* found that HNTs could form liquid phases when were dispersed in water or ionic liquids. They used a liquid crystal self-templating approach and the mechanical shearing method to get the highly aligned nanostructure (Fig. 7). The highly oriented HNTs could be retained over a wide temperature range and that led to a significant improvement and a high anisotropy in the conductivity properties.[32]

2.3. HNT self-assembly induced by an electric force

HNTs are negative and have anisotropic structure, which makes the dipole of the direction parallel to the HNT axis much larger than the direction of the vertical axis. In the effect of an external electric field, the high polarizability makes the HNTs generate alignment. An electric force is applied in the spinning solution during electrospinning, which can induce the preferred alignment of HNTs. Zhao *et al.* fabricated HNT-doped poly(lactic-*co*-glycolic acid) (PLGA) nanofibers using electrospinning. The results showed that the HNTs were distributed in the nanofibers with a coaxial manner and did not have a significant effect on the morphology of the composite nanofibers. Incorporation of HNTs improved the mechanical properties and the composite nanofibers exhibited good biocompatibility.[33] Xue *et al.* prepared electrospun microfiber membranes embedded with drug-loaded HNTs. It was also found that the nanotubes were aligned in the microfibers and the

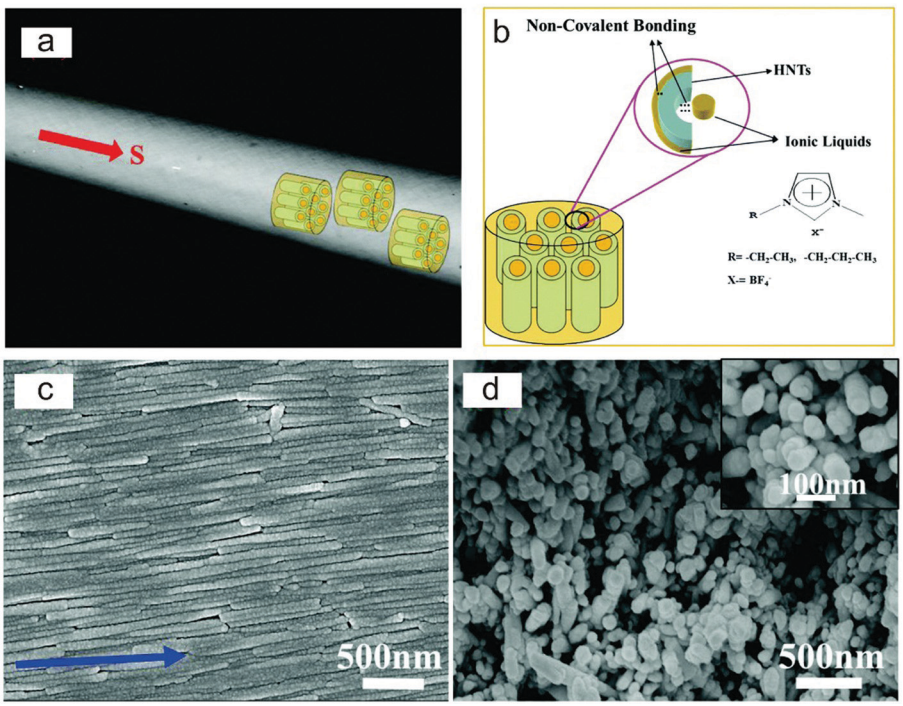

Fig. 7 Liquid crystal self-assembly of ionogels under shear force. (a) Birefringence behaviors brought by oriented HNTs in the ionogels. (b) Schematic illustration of non-covalent bonding between HNTs and the ionic liquid. (c) SEM of the ionogels and (d) their cross section morphology.[32] Copyright 2016, Royal Society of Chemistry.

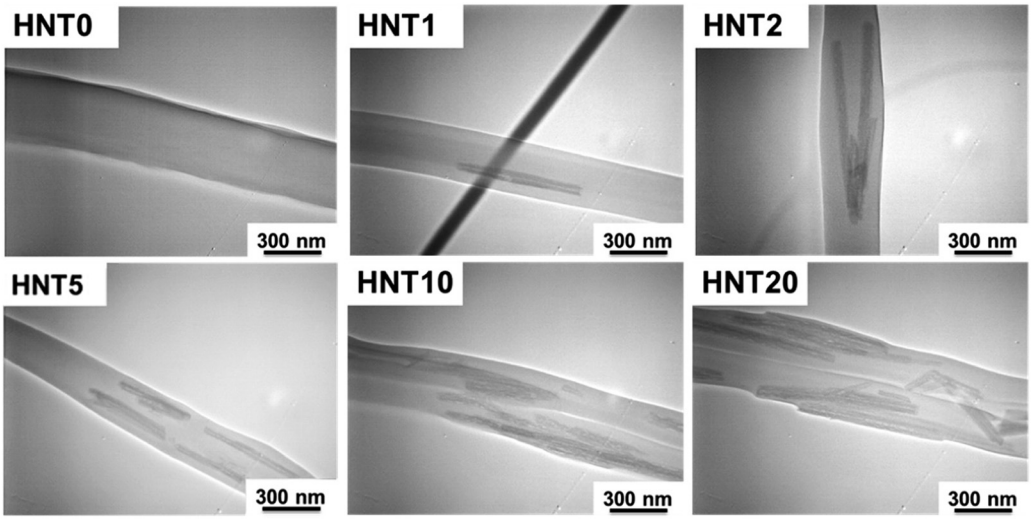

Fig. 8 TEM images of the electrospun microfibers doped with HNTs with different tube contents.[34] Copyright 2015, American Chemical Society.

tensile strength of the membranes was increased with the HNT doped fibers[34] (Fig. 8).

3. HNT assembly on polymeric and biological substrates

3.1. HNT assembly on polymeric substrates

By an immersing and drying method, HNTs can be assembled on various polymeric substrates and bring interesting and practical properties. The negative characteristic, anisotropic structures, massive hydroxyls with good hydrophilicity and excellent stability of HNTs facilitated the coating on polymeric substrates for various applications. For example, it could improve the hydrophilicity, flame-retardant property, separation performance, roughness and other properties.

3.1.1. HNT assembly on polymeric substrates with the aid of dopamine. HNTs have massive hydroxyl groups on their surfaces and good hydrophilicity, which is helpful for cell adhesion. Polylactic acid (PLA) is limited in actual clinical use due to its hydrophobicity, smooth surface and weak cell adhesion. Recently, Wu *et al.* modified 3D printed PLA patterns using a HNT coating with the aid of dopamine. Dopamine could transfer into polydopamine *via* self-polymerization, which can bind to the surfaces of the HNTs and the PLA matrix. After HNT coating, the roughness and hydrophilicity of the scaffolds were significantly increased, which improved the adhesion and viability of cells.[35]

3.1.2. HNT assembly on polymeric substrates by non-covalent interactions. HNTs show high thermal stability and good flame retardancy. The mechanism of flame resistance is that the massive hydroxyl groups of HNTs can condense to produce water under high temperatures. HNTs can be assembled on polymer surfaces to improve the flame-retardant property. Our laboratory prepared high flame-retardant polyurethane foam by dipping the foam into a HNT suspension. It was found that a HNT coating could be formed on the surface of the polyurethane foam uniformly. After the modification, the thermal stability, mechanical properties, and flame retardance were significantly improved.[36]

In the next study, HNTs were first modified by grafting with hexadecyltrimethoxysilane to improve their hydrophobic performance and then their suspension was used to modify polyurethane foam. The hydrophobic HNT modified polyurethane foam not only had good flame retardance but good oil absorption. It was found that the modified HNTs peeled off very little from the foam during use due to the interfacial interactions between the HNTs and polyurethane foam such as hydrogen bonding and van der Waals forces.[37]

Generally, the addition of nanoparticles in nanofiltration membranes can enhance the separation ability. By the strong hydrogen bonds between HNTs and polyvinyl alcohol (PVA), PVA-assisted HNTs were used to modify a nanofiltration membrane with good HNT dispersibility. The HNTs could improve the hydrophilicity and water permeability of the membranes without sacrificing salt retention.[38]

It has been proved that clay minerals can undergo the reaction of electron transfer with some organic molecules. Clay minerals provide sufficient electron accepting sites while organic molecules donate electrons.[39] Zheng *et al.* prepared a supramolecular gel by ultrasound treatment of HNTs and styrene. The research results showed that the free electrons on styrene derived from the conjugated structure can transfer to the aluminium atoms and ferric ions on the crystal edges of the HNTs. With absorption of the polycations of styrene on the HNTs, the mixed HNTs and styrene could form a supramolecular gel in which the HNTs were the gelator (Fig. 9).[40] In the gel, the HNTs are stacked in a cluster state with certain alignment, while there are certain gaps between the HNT clusters. The dry skeleton of nanotubes forms a certain ordered structure, and styrene is fixed in the spacing among the ordered nanotubes. This is a novel and effective approach for preparation of HNT oriented structures.

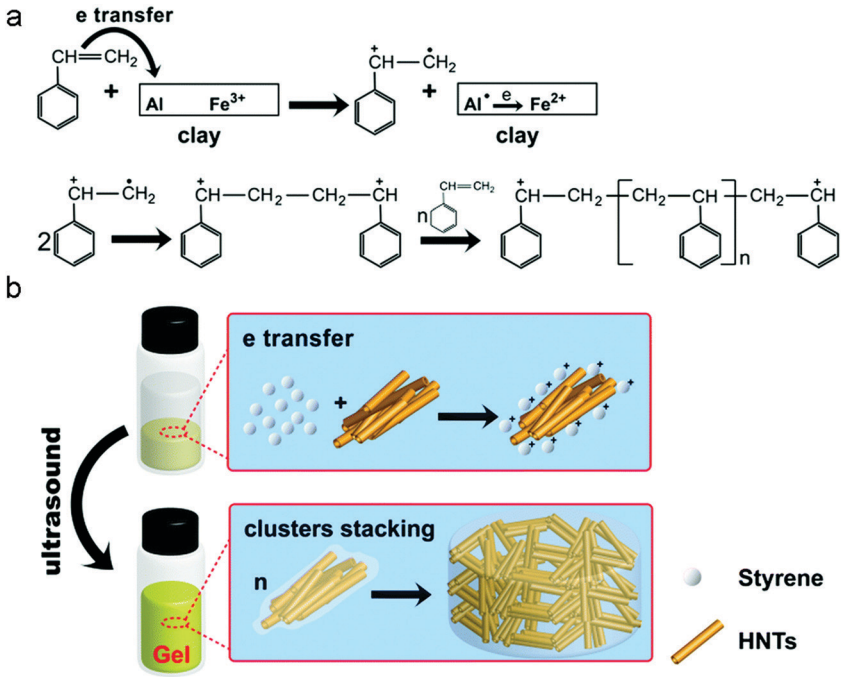

Fig. 9 (a) The electron transfer mechanism between styrene and clay; (b) schematic illustration of the formation of the supramolecular gel.[40] Copyright 2019, Royal Society of Chemistry.

3.1.3. HNT assembly on substrates by the spray-drying method. The spray-drying method is a simple, fast, and effective method for assembling nanoparticles on a substrate. So far, various nanoparticles have been used to modify substrates by spray coating. This method can prepare super-hydrophobic coatings, pH-sensitive self-healing anticorrosion coatings, and functional metal oxide coatings.[41,42] The morphology, roughness and other properties can be controlled by the technological parameters of spray coating. A recent study on controlling the HNT orientation *via* the hydrodynamic flow in a spray coating process was reported. A shear force was exerted on the mixed epoxy/HNT suspension when it flowed through the nozzle exit. The viscosity played an important role in the orientation of the nanotubes. The orientation degree was increased with the increase of the viscosity of the suspension (Fig. 10).[43] Recently, Feng *et al.* first modified HNTs by the hydrolytic condensation of *n*-hexadecyltrimethoxysilane (HDTMS) and tetraethoxysilane (TEOS). The reaction of HDTMS and TEOS could form polysiloxane, which modified the surface of the HNTs during the silanization. The modified HNTs were coated on glass slides, steel, cotton, paper and wood by spraying drying. All the HNT coatings were uniform and did not have significant defects and large aggregates, which demonstrated that it was feasible to use the spray coating process to assemble HNTs on substrates. HNTs randomly distributed on the surfaces of the substrate due to the low viscosity of the dispersion. The surfaces roughness

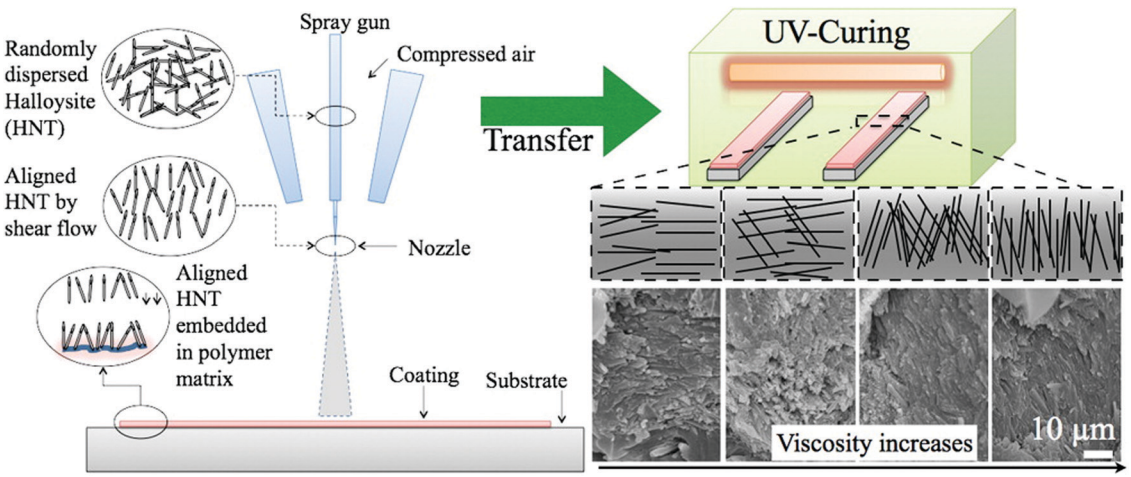

Fig. 10 HNT orientation controlled by the viscosity using the spray coating process,[43] Copyright 2016, American Chemical Society.

of the coating increased with the increase of the silane loading.[41] He *et al.* prepared a HNT coating on glass slides for cell capture. In that study, it was found that the surface roughness and thickness of the HNT coatings increased with the augmentation of the HNT dispersion concentration.[44] Moreover, spray coating is a quick and economic way and environment-friendly modification method for sensor interfaces. By this method, the HNT coating modified surface of a plasmon resonance (SPR) sensor achieved greatly improved sensitivity because the large surface area and high refractive index of the HNT layer significantly increased the probing electric field intensity and hence the measurement sensitivity.[45]

3.2. HNT assembly on biological substrates

3.2.1. HNT assembly on hair. The unique HNT tubular structure with an empty lumen allows it to load drugs or dyes. It is a promising method to color hair or cure diseases which are relevant to hair if HNTs can be self-assembled on hair.[46,47] Panchal *et al.* colored hair using dye-loaded HNTs. Color/drug loaded HNTs could self-assemble on the surfaces of hair by a simple process, *i.e.* dipping the hair strands into the HNT dispersion for 1–5 min (Fig. 11). The hair began to swell when it is wet. Therefore cuticles opened up creating space, which facilitated the penetration of the HNT dispersion. After drying, the cuticles closed down to the initial state and the HNTs were trapped in them. They colored grey hair into a bright orange color by lawsone-loaded HNT treatment successfully (Fig. 11b). After six shampoo–water washing cycles, the color remained, which demonstrated the high stability of the HNT coating. There were hydrogen bonds and van der Waals force interactions between the hair and HNTs, which are responsible for the good stability. Apart from the color, insecticide permethrin was chosen as the drug model and permethrin functionalized HNTs were assembled on hair. It was effective against *C. elegans* nematodes (Fig. 11c and d).[47]

3.2.2. HNT self-assembly on cells. Using cells as the template to construct biological scaffolds was a good strategy for application in microcapsules, microelectrodes, catalysts and adsorbents.[48] Combining with the superiority that HNTs could load a variety of drugs, nutrients, enzymes and nucleic acids into the lumens, cells coated with functionalized HNTs show practical applications. Recently, HNTs as a nanocarrier were used to assemble on the wall of cells or bacteria.[48–50] Konnova *et al.* prepared Fe oxide nanoparticle functionalized-HNTs and then coated them on yeast cells. It had promising application in the separation or delivery of cells.[50] Based on layer-by-layer deposition, HNTs could modify the growth behavior of cells. For example, cationic (poly)allylamine hydrochloride (PAH) could be coated on yeast cells with negative charges and then the cell–PAH composite showed a positive surface, which facilitated negative HNT coating on the cell–PAH composite. In order to prevent mechanical disassembly both PAH and anionic sodium PSS were coated on the cell–PAH–HNT (Fig. 12a and b). The halloysite–polyelectrolyte coated cells are stable for at least two hours, which can find applications in controllable cell growth. After the thermal decomposition of cell–PAH–HNT at high temperature, microcapsules with high porosity could be obtained.[48]

3.2.3. HNT self-assembly on zebrafish embryos. Recently the toxicity study of HNTs on a zebrafish model was reported by our laboratory.[15] HNTs didn't show acute and lethal toxicity in the development of zebrafish. It was attractive that the nanotubes could wrap the surface of the embryo chorion when the concentration reached 25 mg mL^{-1} or higher (Fig. 12c and d). It was hard to confirm that HNTs could accumulate inside

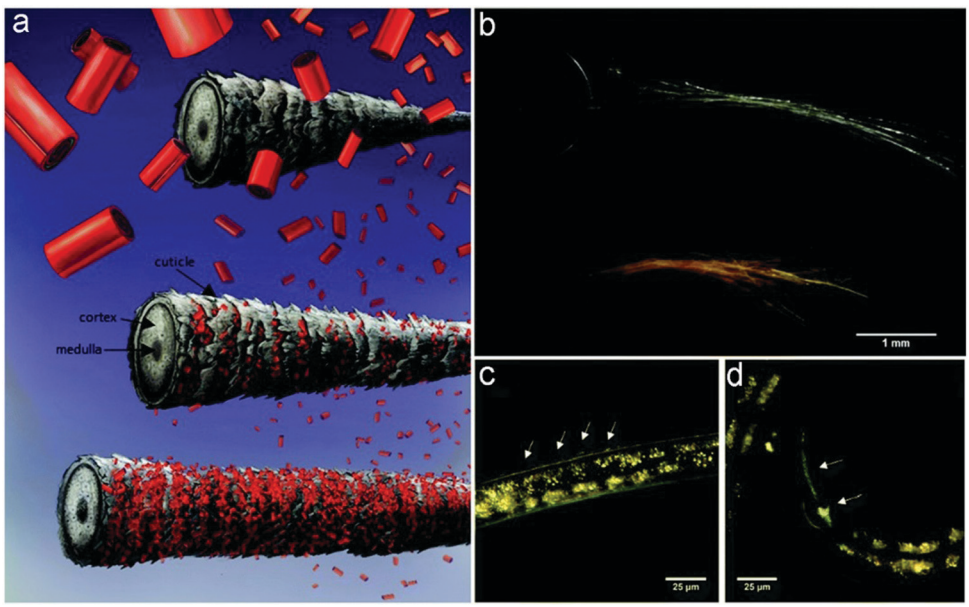

Fig. 11 (a) Preparation of a HNT coating on the surface of hair from anchoring in the cuticle to capillary force/drying driven surface assembly; (b) color difference of the hair before and after HNT self-assembly with the lawsone functional molecule; (c) confirmation of permethrin-loaded HNTs in the cuticle (c) and in the intestines (d) of *C. elegans*, reproduced with permission from ref. 47. Copyright 2018, Royal Society of Chemistry.

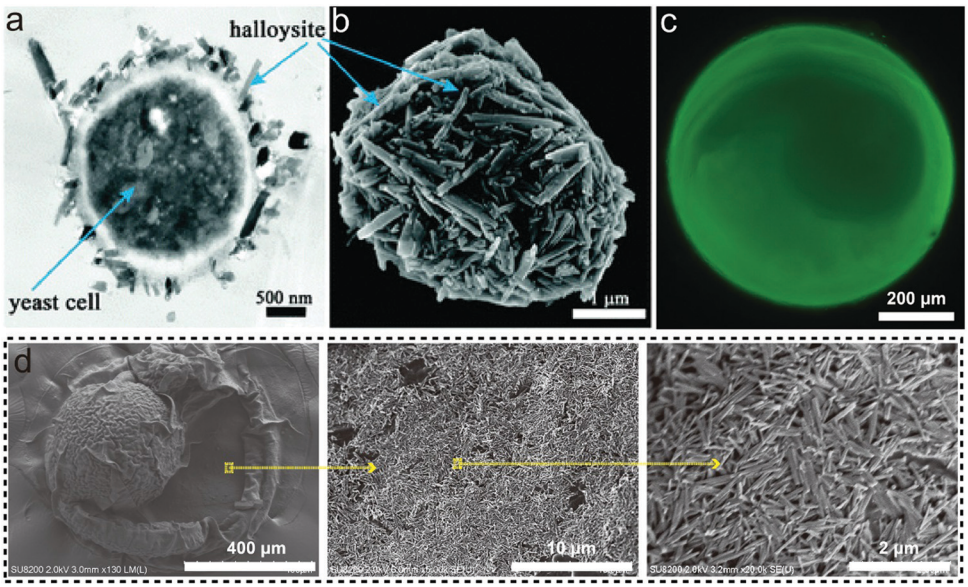

Fig. 12 (a) TEM and (b) SEM of yeast cells coated by modified HNTs.[48] Copyright 2013, Royal Society of Chemistry. (c) Fluorescence microscopy and (d) SEM of HNT self-assembly on zebrafish embryos.[15] Copyright 2018, Royal Society of Chemistry.

the embryos. Single wall carbon nanotube (SWCNT) agglomerates also could adhere to the surface of the embryo chorion and big enough SWCNT agglomerates could not go through the pores in the embryos.[51] So, it was considered that the aggregates of HNTs could not be internalized by the zebrafish embryos possibly.

4. The applications of self-assembly of HNTs in the biomedical field

The micro or nanoscale topography plays an important role in cell behaviors including cell adhesion, migration, proliferation, activation and differentiation. Designing a suitable architecture *via* halloysite assembly can control the cell behavior and find application in different biomedical areas.

4.1. Capture of circulating tumor cells

Metastasis of cancer cells from a primary tumor to distant organs was the main reason that led to poor prognosis. Using functionalized biomaterial surfaces enhanced the efficacy of capturing circulating tumor cells (CTCs), which was an important diagnostic tool for preventing metastasis. However, capture of cancer cells with high purity was challenging in that both CTCs and leukocytes possess selectin ligands. How to choose the CTCs and exclude the leukocytes is key for designing functionalized biomaterial surfaces. Previously, it was reported that different cell types had a dissimilar reaction to HNT exposure.[52–54] Hughes *et al.* prepared HNT coatings with different concentrations and investigated the effects of the coating on leukocyte adhesion. The different concentrations of HNTs allowed tuning the surface roughness. It is found that the HNTs could prevent leukocyte adhesion and spreading. Moreover, they extend a study of leukocyte spreading on different surface roughness. The surface roughness characteristics controlled the cell behaviors by determining the average distance between discrete surface features correlated with adhesion metrics. Below a threshold concentration, leukocyte spreading on the HNT coating became comparable to smooth surfaces.[52] Moreover, they developed a microscale flow device with a functionalized surface of E-selectin and antibody molecules and a HNT coating. The E-selectin and antibody molecules facilitated the selective capture of CTCs and increased the capture efficiency and purity. The HNT coating could increase the surface area onto which molecules could adsorb and enhance the adhesion of CTCs.[53]

Generally, EpCAM antibody conjugated surfaces as the gold standard for CTC specific isolation were used. In the absence of EpCAM, Mitchell *et al.* exploited the possibility of a HNT based surface functionalized by surfactant (sodium dodecanoate, NaL). After the modification with NaL, the negative charge and dispersion stability of the HNTs increased. Then, NaL–HNT was assembled on the inner microrenathane surface to form the coating. Surfactant functionalized nanotube coated surfaces enhanced the absorption of E-selectin (ES) and increased the roughness. The roughened surfaces after the modification with the NaL–HNT coating could induce a switch from E-selectin mediated rolling to firm tumor adhesion under flow.[55] In addition, Mitchell's laboratory compared the response difference of cells on HNTs modified by cationic (decyltrimethylammonium bromide, DTAB) and anionic surfactants. It was interesting that NaL-functionalized HNTs improved the tumor cell adhesion while negating leukocyte adhesion but DTAB treated HNTs abolished tumor cell capture while promoting leukocyte adhesion (Fig. 13).[56]

We have also investigated the effects of HNT assembled structures on the capture of cancer cells. A patterned surface with ordered alignment of the nanotubes was prepared using a capillary tube device *via* evaporation-induced HNT assembly (Fig. 5a). Tumor cells exhibited extended pseudopodia on the patterned HNT coating but had a rounded conformation on the

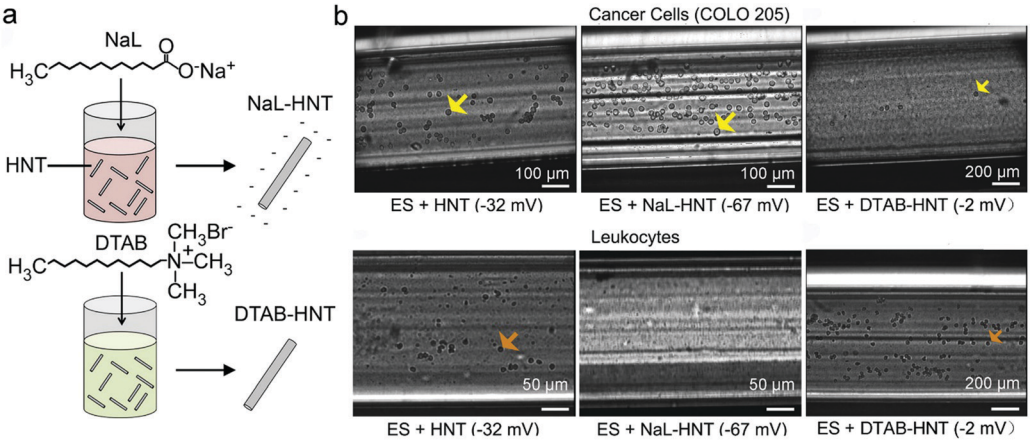

Fig. 13 (a) Schematic illustration of HNTs functionalized by NaL and DTAB; (b) cancer cell and leukocyte adhesion on the plastic tube surface coated with ES + HNTs, ES + NaL–HNT and ES + DTAB–HNT, reproduced with permission from ref. 56. Copyright 2015, Elsevier.

smooth glass surface. The Neuro-2a cell capture efficiency on the HNT coating was more than 1.7, 1.4, and 6.2 times compared to blank glass after the cells' incubation for 1 h, 2 h and 3 h, respectively. These differences arose from the HNT coating showing higher surface roughness than the blank glass. The preparation process of the device was simple and the captured cells are easy to stain and count.[20] Another example was that HNT patterns coated a glass substrate using a device with a slit-like confined space and were further conjugated with anti-EpCAM (Fig. 5b). As shown in Fig. 14a–c, the HNT coating captured more MCF-7 cells than the smooth glass substrate and the HNT coating with a concentration of 2% was better for cell capture. From Fig. 14d and e MCF-7 cells had the bigger spreading areas on the HNT coating than blank glass.[27] A high capture efficiency of tumor cells can also be achieved by a HNT coating fabricated by the thermal spraying method. Furthermore, HNTs were loaded with anticancer drug doxorubicin and then thermally sprayed into coatings. The MCF-7 cells captured on the DOX loaded HNT coating exhibited significant membrane rupture characteristics and only 3% cell viability after 16 h. All these results suggested that the assembled HNT pattern shows promising applications in clinical circulating tumor cell capture for early diagnosis as an implantable therapeutic device for preventing tumor metastasis.[44]

4.2. Guiding cell orientation

Cell can recognize and respond to the substrate, so the morphological and chemical characteristics of the substrate play an important role in the cell behavior. It is suggested that anisotropic structures could induce cell orientation.[57,58] HNTs as one-dimensional nanoparticles can be the building block, which could assemble into an anisotropic structure under shear force. Recently, aligned HNTs on solid substrates were fabricated by a shearing method with brush assistance (Fig. 6). The oriented HNTs could induce human foreskin fibroblast (HFF) and human mesenchymal stem cell (HBMSC) orientation. Further, orientation of HBMSC helped osteogenic differentiation.[11] We have also prepared a HNT coating with concentric ring patterns by evaporation-induced self-assembly and investigated the cell behavior on the coating. It was attractive that the HNT rings could direct the orientation of C2C12 myoblast cells perpendicular to the rings.[19] Wu *et al.* designed HNT coated PLA patterns with different stripe widths. The stripe width of the PLA pattern affected the cell morphology and the best orientation of cells was found at a stripe width of 0.05 mm (Fig. 15).[35] This simple method of managing the cell orientation has potential in tissue engineering scaffolds and biosensors.

4.3. Biosensors

HNTs could modify sensors to improve the sensitivity, which is helpful for detection of biochemical species.[45,59] The performance of SPR sensors before and after modification using HNT coatings was compared to detect the resonance wavelength shift when flowing through phosphate buffer and bovine serum albumin solutions (Fig. 16a). The sensitivity of the sensors was enhanced 1.9 and 7.1-fold in the groups modified by the 2.5% and 5% concentration of HNTs, respectively.[45] A HNT based substrate was also used for CTC capture, in which it is usual to compare the capture efficacy by cell staining. We are now working on development of a HNT coated optical fiber and design of a novel biosensor for tumor cells. When the tumor cell suspension flows through the optical fiber with the HNT coating, cells were captured by the optical fiber and a spectral signal could respond to the changes (Fig. 16b). This method was simple, effective, and low-cost, while the captured cells could stay alive for further study.

4.4. Others

Self-assembled structures of HNTs also show promising applications such as drug release, wound healing, healthcare and hemostasis.[60–62] Lvov *et al.* made HNTs assemble on hair, loading a drug or dye which could color the hair and also could prevent disease which was relevant to hair.[47] Zhang *et al.* incorporated metronidazole-loaded HNTs into electrospun nanofibers, which could extend the release of metronidazole. The sustained release of metronidazole could prevent the colonization of anaerobic fusobacteria.[34] Wu *et al.* coated

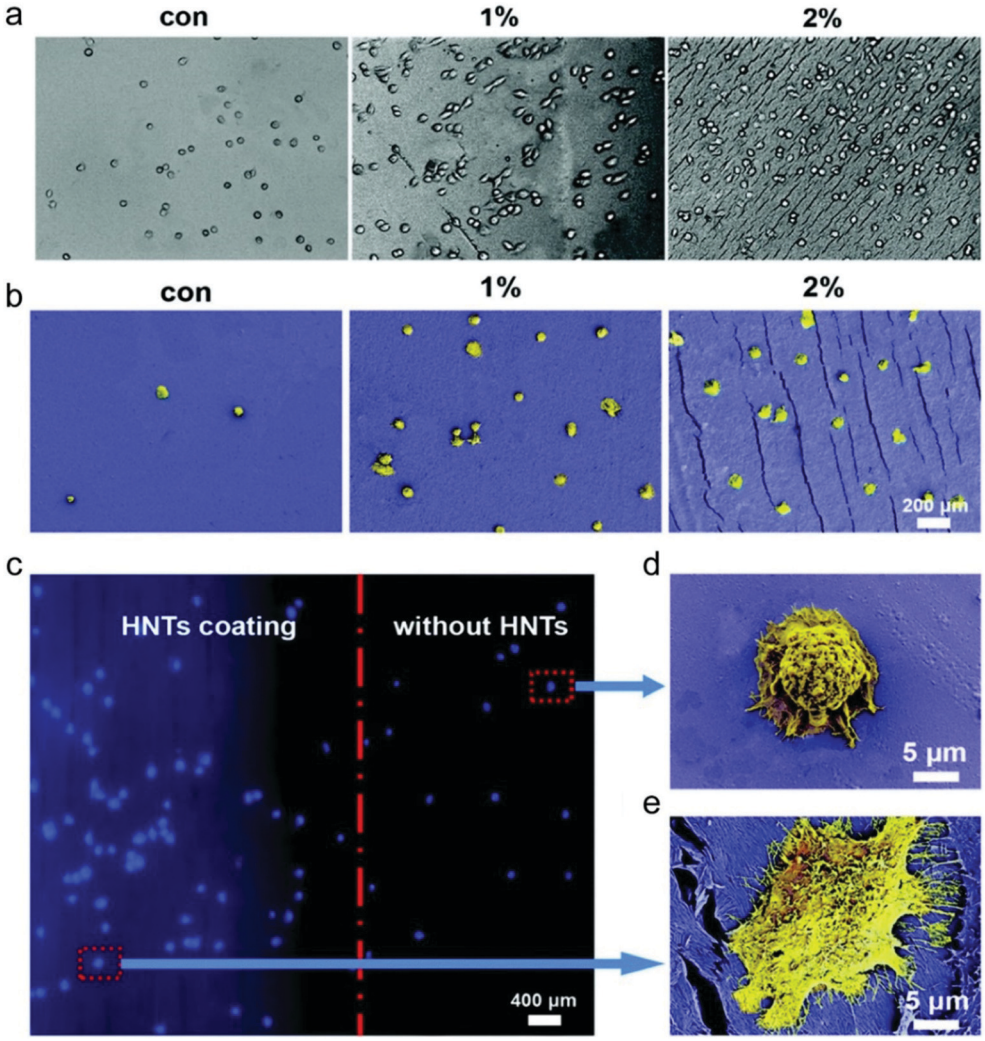

Fig. 14 Optical images (a) and SEM images (b) of captured MCF-7 cells on a blank glass surface and substrate with a HNT coating, 1% and 2% represent the concentrations of HNTs; (c) DAPI staining of the MCF-7 cells captured on the HNT coating and blank glass substrate; SEM images of the cell morphology on blank glass (d) and the HNT coatings (e), reproduced with permission from ref. 27, Copyright 2017, Royal Society of Chemistry.

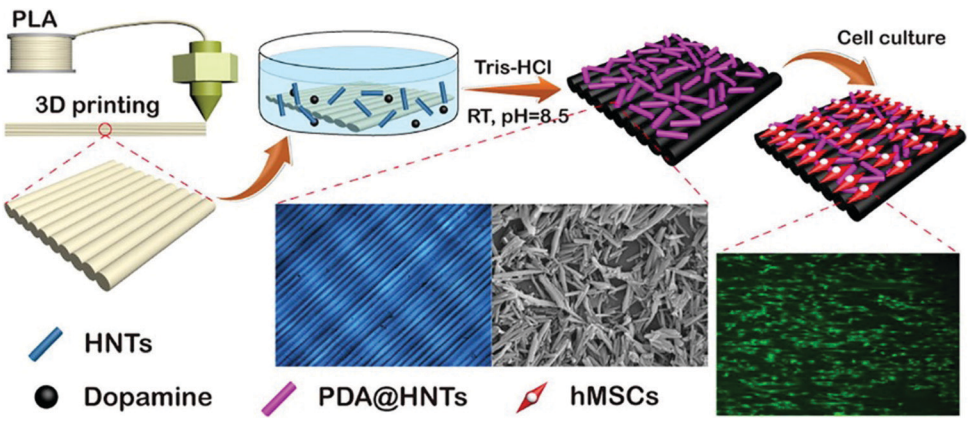

Fig. 15 Schematic illustration of preparation of HNT coated PLA patterns and and induced cell orientation.[35] Copyright 2018, Elsevier.

chlorhexidine gluconate-loaded HNTs on fabric by using the dip-coating method. Chlorhexidine gluconate/HNT coated fabric exhibited significant antibacterial activity and no stimulation to the skin of rabbits. It was promising that the chlorhexidine gluconate/HNT coated fabric was used as an antibacterial material.[61]

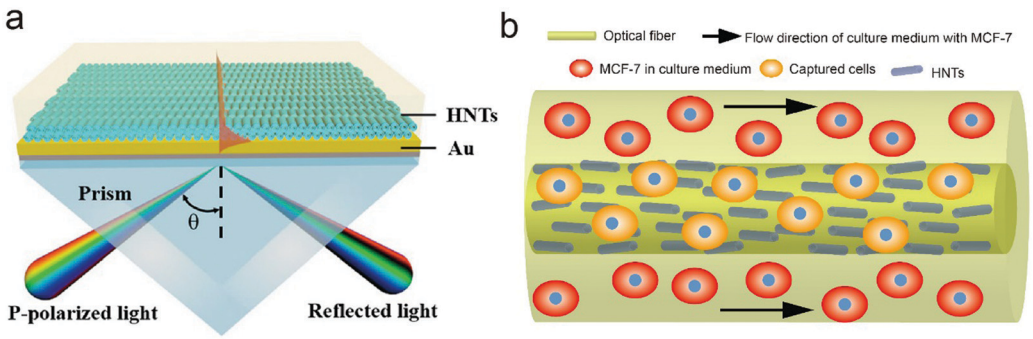

Fig. 16 Application of self-assembly of HNTs on biological sensors. (a) Schematic illustration of SPR modified by HNTs,[45] Copyright 2018, American Chemical Society. (b) Schematic illustration of an optical fiber sensor functionalized by HNTs for cell capture, unpublished.

5. Conclusion and outlook

This review summarized the recent progress in HNT self-assembly and applications in the biomedical field. The unique properties of HNTs such as a large aspect ratio, high dispersion ability, opposite charges on the inner/outer surface, and good hydrophilicity allow HNT assembly using various methods. First, HNT self-assembly methods including solvent evaporation, shear force, and electric force were introduced. Then, HNT assembly on polymeric substrates and biological substrates by van der Waals interaction forces and hydrogen bond interactions was discussed in detail. This assembled halloysite structures have attractive properties such as oriented structure, bigger roughness, good hydrophilicity, excellent flame-retardant abilities, improved oil–water separation and so on. Finally, self-assembled HNT coatings applied in the biomedical field were emphasized. Shear force and solvent evaporation induced HNT orientation could induce cell orientation and cell differentiation. It was promising to modify tissue engineering scaffolds using HNT coatings. HNT coatings *via* solvent evaporation helped cell adhesion. CTCs on self-assembled HNT coatings exhibited higher adhesion ability due to the material–cell interactions.

In the future, development of more self-assembly methods is expected such as magnetic field induced alignment of HNTs for biomedical applications. Magnetic nanoparticles can be aligned into ordered structures in a magnetic field. The lumen of HNTs is possible to use for loading Fe_2O_3 or other magnetic nanoparticles. Using micron-scale channels as a template for ordered HNT structures is an alternative method, involving dropping the nanoparticle dispersion into the micron-scale channels and then evaporating the solvent in a vacuum. Then a HNT pattern parallel to the channels can be formed. Moreover, preparation of self-assembled HNT coatings on a 3D substrate is of great significance to 3D tissues such as nerves, bones, skin, and muscles with anisotropic architecture for retaining their physiological functions. Construction of 3D tissue engineering scaffolds with oriented HNTs by self-assembly is a good strategy for tissue repair. In addition, it is desirable to design optical devices using aligned HNT coated optical fibers for real-time detection of disease signals. Of course, the practical application of halloysite based drug delivery and hemostatic products in the clinic is most urgent. With more efforts being made, it is definitely sure that broader applications of HNT assembled structures in biomedical areas will be realized.

Conflicts of interest

There are no conflicts to declare.

Acknowledgements

This work was supported by the grants from Guangdong Basic and Applied Basic Research Foundation (2019A1515011509), and the Fundamental Research Funds for the Central Universities (21619102).

References

1 Y. Xia, P. Yang, Y. Sun, Y. Wu, B. Mayers, B. Gates, Y. Yin, F. Kim and H. Yan, *Adv. Mater.*, 2003, **15**, 353–389.
2 E. Joussein, S. Petit, J. Churchman, B. Theng, D. Righi and B. Delvaux, *Clay Miner.*, 2005, **40**, 383–426.
3 M. Liu, Z. Jia, D. Jia and C. Zhou, *Prog. Polym. Sci.*, 2014, **39**, 1498–1525.
4 X. Zhao, Q. Wan, X. Fu, X. Meng, X. Ou, R. Zhong, Q. Zhou and M. Liu, *ACS Sustainable Chem. Eng.*, 2019, **7**, 18965–18975.
5 M. Massaro, G. Lazzara, S. Milioto, R. Noto and S. Riela, *J. Mater. Chem. B*, 2017, **5**, 2867–2882.
6 M. Liu, Y. Shen, P. Ao, L. Dai, Z. Liu and C. Zhou, *RSC Adv.*, 2014, **4**, 23540–23553.
7 M. Massaro, G. Cavallaro, C. G. Colletti, G. Lazzara, S. Milioto, R. Noto and S. Riela, *J. Mater. Chem. B*, 2018, **6**, 3415–3433.
8 R. F. Fakhrullin and Y. M. Lvov, *Nanomedicine*, 2016, **11**, 2243–2246.
9 L. Meng, R. Bian, C. Guo, B. Xu, H. Liu and L. Jiang, *Adv. Mater.*, 2018, **30**, 1706938.
10 Q. Yang, C. Xiao, W. Chen, A. Singh, T. Asai and A. Hirose, *Diamond Relat. Mater.*, 2003, **12**, 1482–1487.
11 X. Zhao, C. Zhou, Y. Lvov and M. Liu, *Small*, 2019, **15**, 1900357.

12 X. Zan, S. Feng, E. Balizan, Y. Lin and Q. Wang, *ACS Nano*, 2013, **7**, 8385–8396.
13 M. Nakayama, S. Kajiyama, A. Kumamoto, T. Nishimura, Y. Ikuhara, M. Yamato and T. Kato, *Nat. Commun.*, 2018, **9**, 568.
14 Y. Zhao, G. Cavallaro and Y. Lvov, *J. Colloid Interface Sci.*, 2015, **440**, 68–77.
15 Z. Long, Y.-P. Wu, H.-Y. Gao, J. Zhang, X. Ou, R.-R. He and M. Liu, *J. Mater. Chem. B*, 2018, **6**, 7204–7216.
16 G. I. Fakhrullina, F. S. Akhatova, Y. M. Lvov and R. F. Fakhrullin, *Environ. Sci.: Nano*, 2015, **2**, 54–59.
17 M. Liu, R. Fakhrullin, A. Novikov, A. Panchal and Y. Lvov, *Macromol. Biosci.*, 2019, **19**, 1800419.
18 G. Cavallaro, G. Lazzara, S. Milioto, G. Palmisano and F. Parisi, *J. Colloid Interface Sci.*, 2014, **417**, 66–71.
19 M. Liu, Z. Huo, T. Liu, Y. Shen, R. He and C. Zhou, *Langmuir*, 2017, **33**, 3088–3098.
20 M. Liu, R. He, J. Yang, W. Zhao and C. Zhou, *ACS Appl. Mater. Interfaces*, 2016, **8**, 7709–7719.
21 E. Tarasova, E. Naumenko, E. Rozhina, F. Akhatova and R. Fakhrullin, *Appl. Clay Sci.*, 2019, **169**, 21–30.
22 R. D. Deegan, O. Bakajin, T. F. Dupont, G. Huber, S. R. Nagel and T. A. Witten, *Nature*, 1997, **389**, 827–829.
23 D. Mampallil and H. B. Eral, *Adv. Colloid Interface Sci.*, 2018, **252**, 38–54.
24 P. J. Yunker, T. Still, M. A. Lohr and A. Yodh, *Nature*, 2011, **476**, 308–311.
25 L. Qin, Y. Zhao, J. Liu, J. Hou, Y. Zhang, J. Wang, J. Zhu, B. Zhang, Y. Lvov and B. Van der Bruggen, *ACS Appl. Mater. Interfaces*, 2016, **8**, 34914–34923.
26 X. Liang, L. Qin, J. Wang, J. Zhu, Y. Zhang and J. Liu, *Ind. Eng. Chem. Res.*, 2018, **57**, 3235–3245.
27 R. He, M. Liu, Y. Shen, Z. Long and C. Zhou, *J. Mater. Chem. B*, 2017, **5**, 1712–1723.
28 Z. Fan and S. G. Advani, *Polymer*, 2005, **46**, 5232–5240.
29 Y. J. Cha and D. K. Yoon, *Adv. Mater.*, 2017, **29**, 1604247.
30 S.-M. Chen, H.-L. Gao, Y.-B. Zhu, H.-B. Yao, L.-B. Mao, Q.-Y. Song, J. Xia, Z. Pan, Z. He and H.-A. Wu, *Natl. Sci. Rev.*, 2018, **5**, 703–714.
31 S. Park, G. Pitner, G. Giri, J. H. Koo, J. Park, K. Kim, H. Wang, R. Sinclair, H. S. P. Wong and Z. Bao, *Adv. Mater.*, 2015, **27**, 2656–2662.
32 N. Zhao, Y. Liu, X. Zhao and H. Song, *Nanoscale*, 2016, **8**, 1545–1554.
33 Y. Zhao, S. Wang, Q. Guo, M. Shen and X. Shi, *J. Appl. Polym. Sci.*, 2013, **127**, 4825–4832.
34 J. Xue, Y. Niu, M. Gong, R. Shi, D. Chen, L. Zhang and Y. Lvov, *ACS Nano*, 2015, **9**, 1600–1612.
35 F. Wu, J. Zheng, Z. Li and M. Liu, *Chem. Eng. J.*, 2019, **359**, 672–683.
36 F. Wu, J. Zheng, X. Ou and M. Liu, *Macromol. Mater. Eng.*, 2019, 1900213.
37 W. Fan, K. Pickett, A. Panchal, M. Liu and Y. M. Lvov, *ACS Appl. Mater. Interfaces*, 2019, **11**, 25445–25456.
38 L. Jia, X. Zhang, J. Zhu, S. Cong, J. Wang, J. Liu and Y. Zhang, *Environ. Sci.: Water Res. Technol.*, 2019, **5**, 1412–1422.
39 D. Solomon, *Clays Clay Miner.*, 1968, **16**, 31–39.
40 J. Zheng, X. Ou, F. Wu and M. Liu, *Chem. Commun.*, 2019, **55**, 10756–10759.
41 K. Feng, G.-Y. Hung, J. Liu, M. Li, C. Zhou and M. Liu, *Chem. Eng. J.*, 2018, **331**, 744–754.
42 X. Lin, Y. Zeng, X. Zhou and C. Ding, *Mater. Sci. Eng., A*, 2003, **357**, 228–234.
43 K. Song, R. Polak, D. Chen, M. F. Rubner, R. E. Cohen and K. A. Askar, *ACS Appl. Mater. Interfaces*, 2016, **8**, 20396–20406.
44 R. He, M. Liu, Y. Shen, R. Liang, W. Liu and C. Zhou, *Mater. Sci. Eng., C*, 2018, **85**, 170–181.
45 M. Yang, X. Xiong, R. He, Y. Luo, J. Tang, J. Dong, H. Lu, J. Yu, H. Guan, J. Zhang, Z. Chen and M. Liu, *ACS Appl. Mater. Interfaces*, 2018, **10**, 5933–5940.
46 A. C. Santos, A. Panchal, N. Rahman, M. Pereira-Silva, I. Pereira, F. Veiga and Y. Lvov, *Nanomaterials*, 2019, **9**, 903.
47 A. Panchal, G. Fakhrullina, R. Fakhrullin and Y. Lvov, *Nanoscale*, 2018, **10**, 18205–18216.
48 S. A. Konnova, I. R. Sharipova, T. A. Demina, Y. N. Osin, D. R. Yarullina, O. N. Ilinskaya, Y. M. Lvov and R. F. Fakhrullin, *Chem. Commun.*, 2013, **49**, 4208–4210.
49 Y. Lvov, A. Aerov and R. Fakhrullin, *Adv. Colloid Interface Sci.*, 2014, **207**, 189–198.
50 S. Konnova, Y. Lvov and R. Fakhrullin, *Clay Miner.*, 2016, **51**, 429–433.
51 J. Cheng, E. Flahaut and S. H. Cheng, *Environ. Toxicol. Chem.*, 2007, **26**, 708–716.
52 A. D. Hughes, G. Marsh, R. E. Waugh, D. G. Foster and M. R. King, *Langmuir*, 2015, **31**, 13553–13560.
53 A. D. Hughes, J. Mattison, L. T. Western, J. D. Powderly, B. T. Greene and M. R. King, *Clin. Chem.*, 2012, **58**, 846–853.
54 A. D. Hughes and M. R. King, *Langmuir*, 2010, **26**, 12155–12164.
55 M. J. Mitchell, C. A. Castellanos and M. R. King, *J. Biomed. Mater. Res., Part A*, 2015, **103**, 3407–3418.
56 M. J. Mitchell, C. A. Castellanos and M. R. King, *Biomaterials*, 2015, **56**, 179–186.
57 M. Li, X. Fu, H. Gao, Y. Ji, J. Li and Y. Wang, *Biomaterials*, 2019, **216**, 119269.
58 N. Masoumi, B. L. Larson, N. Annabi, M. Kharaziha, B. Zamanian, K. S. Shapero, A. T. Cubberley, G. Camci-Unal, K. B. Manning and J. E. Mayer Jr, *Adv. Healthcare Mater.*, 2014, **3**, 929–939.
59 G. Jia, Z. Huang, Y. Zhang, Z. Hao and Y. Tian, *J. Mater. Chem. C*, 2019, **7**, 3843–3851.
60 Y. Wu, J. Yang, H. Gao, Y. Shen, L. Jiang, R. Zhou, F. Li, R. He and M. Liu, *ACS Appl. Nano Mater.*, 2018, **1**, 595–608.
61 Y. Wu, Y. Yang, H. Liu, X. Yao, F. Leng, Y. Chen and W. Tian, *RSC Adv.*, 2017, **7**, 18917–18925.
62 M. Massaro, G. Buscemi, L. Arista, G. Biddeci, G. Cavallaro, F. D'Anna, F. D. Blasi, A. Ferrante, G. Lazzara, C. Rizzo, G. Spinelli, T. Ullrich and S. Riela, *ACS Med. Chem. Lett.*, 2019, **10**, 419–424.